Swift Mini-Survey of SDSS [OIII] AGN with Swift:

Testing the Hypothesis That $L_{[OIII]}$ Traces AGN Luminosity

L. Angelini[a], I. M. George[a,b], J. Hill[c], C. A. Padgett[a,d], R. F. Mushotzky[a]

[a]NASA/Goddard Space Flight Center, Greenbelt, MD 20771, USA, [b]University of Maryland Baltimore County, Baltimore, MD, 21250, USA, [c]Universities Space Research Association, Columbia, MD 21044, USA, [d]R.S. Information Systems, McLean, VA 22102, USA.

Introduction & Overview

The number of AGN and their luminosity distribution are crucial parameters for our understanding of the AGN phenomenon. Recent work (e.g., Ferrarese and Merritt 2000) strongly suggests every massive galaxy has a central black hole. However, most of these objects either are not radiating or have been very difficult to detect.

We are now in the era of large surveys, and the luminosity function (LF) of AGN has been estimated in various ways. In the X-ray band, *Chandra* and *XMM* surveys (e.g., Barger et al. 2005; Hasinger, et al. 2005) have revealed that the LF of *hard X-ray selected AGN* shows a strong luminosity-dependent evolution with a dramatic break towards low L_X (at all z). This is seen for all types of AGN, but is stronger for the broad-line objects (e.g., Steffen et al. 2004). In sharp contrast, the local LF of *optically-selected samples* shows no such break and no differences between narrow and broad-line objects (Hao et al. 2005).

If, as been suggested, hard X-ray and optical emission line can both be fair indicators of AGN activity, it is important to first understand how reliable these characteristics are if we hope to understand the apparent discrepancy in the LFs.

The SDSS and *Swift*

The Spectroscopic data from the Sloan Digital Sky Survey (SDSS) provides a rich resource for detecting & studying the properties of AGN. Several large & detailed such studies have already been performed by the MPA/JHU group led by Kauffmann.

We present the results from a simple comparison between two "classic" indicators of AGN activity - the luminosity of the [OIII] emission line ($L_{[OIII]}$), and that in the X-ray band (L_X). Unified schemes predict a simply linear relationship between $L_{[OIII]}$ and L_X and such a relationship has been suggested in several studies (e.g., Kraemer et al. 2004; Heckman et al. 2005, Ptak et al. 2006, Netzer et al. 2006; Panessa et al. 2006).

We recognize neither are perfect indicators. Indeed one of our motivations was to study the scatter around any relationship. For $L_{[OIII]}$, we have used data from a subset of SDSS AGN catalog kindly made public by the MPA Team. For L_X with have used data collected by the XRT onboard *Swift*. Through both pointed and serendipitous observations, *Swift* provides a shallow but wide survey complementary to other X-ray surveys.

About *Swift*

Swift is a dedicated satellite to detect Gamma Ray Bursts and their afterglows. The initial detection of the GRB is made with the BAT detector. The satellite then slews and starts observing with the UVOT (optical/UV) and XRT (0.3-10) keV detectors. The typical *Swift* observing strategy for a GRB/afterglow consists of a cluster of snapshots. Depending on the evolution of the flux, the sensitivity of each instrument, and the required science, the same object may be observed several times as for in a monitoring campaign. The satellite on average monitors the same position for about a month. While waiting for new GRBs or return to a position constrain by the sun, *Swift* observes "fill-in" targets. This sample of sources is selected using all the observations made with the XRT on *Swift* when operation with the Photon Counting mode which provides image and spectral information.

Sample Selection

There are 88178 objects in the DR4 releae of the MPA/JHU AGN catalog (http://www.mpa-garching.mpg.de/SDSS/). These were cross-correlated with all *Swift* observations taken up to May 2007. This resulted in 3709 objects within the XRT field of view (20 arcmin). Further screening excludes a few objects with a problematic [OIII] measurement, and all exposures <1ks in PC mode. We also exclude all objects that do not satisfy the conservative emission line ratio criteria to be indicative of AGN activity outlined by Kewley et al. (2001), objects with a redshift z>0.1, and those >10 arcmin from the XRT nominal pointing position. Finally, here we only include objects for which the sum of the exposure [illegible] This gives a **sample of 108 objects** [illegible] **of 358** [illegible] **ons.**

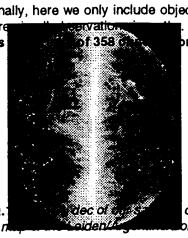

Fig. [illegible] *overlaid on the N_H* [illegible] *survey.*

All data were calibrated and screened using the latest procedures. routine part of the Swift software and the latest calibration data. For each observation, an image and an exposure vignetted corrected map were calculated. All images and exposure maps related to a specific SDSS object were summed. A sliding box detection algorithm was then run on the summed images. For all sources the final rate or upper limit were calculated using an extraction region corresponding to the 90% of PSF, the exposure derived from the vignetted corrected exposure map and the background considering a source free near by the object. The detected or upper limit rates were converted into intrinsic flux by using a power law spectrum of 1.9 and the galactic absorption obtained from the Leiden/Argentina/Bonn survey

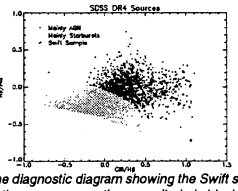

Fig.2: *Line diagnostic diagram showing the Swift sample in red, the other sources meeting our criteria in black, and the other sources in the MPA/JHU AGN catalog in grey.*

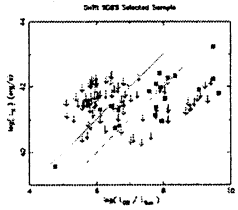

Fig.3: *The $L_{[OIII]}$-L_X plane for the sample. The 20 sources detected at >95 % confidence are shown as the blue squares. 3σ upper limits are shown for the others. The solid & dashed lines are the mean correlations for Seyfert 1s & 2s (respectively) found by Heckman etal (2005).*

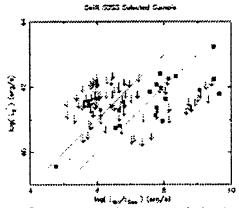

Fig.4: *As for Fig. 3, except the sources judged to have both a strong non-thermal continuum and strong* [OIII] *emission line are shown in red, and those with a weak non-thermal continuum &* [OIII] *line in blue. Intermediate objects are shown in black.*

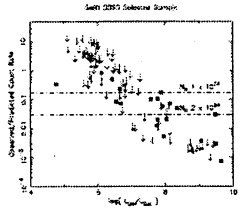

Fig.5: *The observed/predicted count rates assuming $L_{[OIII]}/L_X$=0.02 (from Kraemer et al. 2004), and using the same color scheme as Fig. 3. The effect of additional absorption intrinsic to the AGN is shown be the dashed horizontal lines.*

Example Datasets

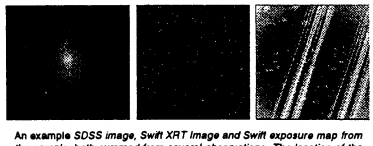

An example SDSS image, Swift XRT image and Swift exposure map from the sample, both summed from several observations. The location of the SDSS source is indicated by the mall circle, and clearly detected. The larger circles are used to estimate the background. The exposure map exhibit many artifacts of the detector, all of which are taken into account during the analysis.

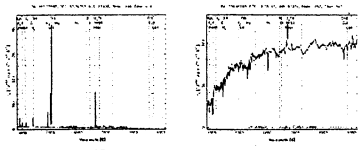

Example SDSS spectra from our sample indicating an object with a strong emission, and an object with both a weak continuum and emission lines.

Caveat

We stress that the values of $L_{[OIII]}$ used here are the (extinction-corrected) luminosities supplied in the MPA/JHU catalog. We have not made any attempt to correct and fit the SDSS spectra ourselves.

Preliminary Results

- We detect 20/108 of the sources in the sample
- These sources cover the full range of $L_{[OIII]}$ of the sample population ($L_{[OIII]}$ ~10^{5}-- 10^{10} L_{sun}) **[Fig. 3]**
- The detected sources exhibit a clear correlation between $L_{[OIII]}$ and L_X in agreement with previous results **[Fig. 3]**
- However there is ~1 order of magnitude scatter in the $L_{[OIII]}/L_X$. **[Figs. 3 & 5]**
- Broadly speaking it appears our predicted vales of L_X were approximately 1 order of magnitude too high **[Fig. 5]**
- The scatter in $L_{[OIII]}/L_X$ is likely to be much larger than a factor 10, given the tight upper limits on some of the objects (particularly apparent for the objects with $L_{[OIII]}$ >10^{8} L_{sun}) **[Fig. 3]**

We have also judged (somewhat qualitatively at this stage) the strength of both the non-thermal continuum and [OIII] emission line in each object in the sample.

- We find **no clear trend** whereby (say) the objects with very strong continuum & lines are preferentially detected. **[Fig. 4].**

(At this stage)
- We find no clear evidence that the detected objects are correlated with any other parameters associated with the AGN or host galaxy (e. g., velocity dispersion, redshift, etc.)

Likely Complications

- Intrinsic reddening and absorption in both the optical and X-ray band. The reddening can be difficult to model for a variety of reasons. Regarding the latter, there are generally too few counts in the current Swift data to allow meaningful spectral analysis in the X-ray band [but see Fig.5].
- Despite our conservative selection criteria, it is possible that star-forming regions & LINERs contribute to $L_{[OIII]}$ in some objects [see Fig. 2].
- Some of the variance in $L_{[OIII]}$ could be due to geometrical considerations associated with non-spherical and/or clumpy [OIII] emission regions
- There appears to be a difference in the $L_{[OIII]}/L_X$ relationship between Seyfert 1s & Seyfert 2s (e.g., Heckman et al. 2005). We have not distinguished between these two classes so far.
- Many AGN are known to exhibit spectral complexity in the X-ray band (such as intense photoionized emission lines in the soft band, "Compton humps," etc.), rather than the simple powerlaw assumed here.
- Time-variability effects: the calculated value of L_X is an "instantaneous" measurement, but $L_{[OIII]}$ represents the average (historic) AGN activity over the previous ~10^{3} years.
- The automated extraction routines necessary for the production of the SDSS catalog can be challenged by the weakness of the lines in some objects (e.g., the right-hand example shown below).

Conclusion & Future Work

Swift is proving to be a valuable resource for more than just GRB research. Here we have taken advantage of the isotropic distribution of GRBs to conduct a relatively unbiased study of the isotropic distribution of AGN.

We conclude that $L_{[OIII]}$ alone is unlikely to provide a robust prediction of the X-ray luminosity in AGN (and vice versa). At the current time, the limited parameter-space investigated does tell us why this is.

We intend follow-up X-ray observations for the detected sources to determine the spectra.

We plan to extend this analysis so as to include more sources as both the *Swift* and SDSS archives grow. We also plan to extend our study to include other parameters associated with the AGN and host galaxy.

References

Barger, A., et al., 2005, AJ., 129, 578 [B05]
Ferrarese, L. & Merrit, D., 2000, ApJ., 539, L9
Hao, L., et al., 2005, A.J., 129, 1795
Hasinger., G., et al., 2005, A&A, 441, 417
Heckman, T., et al., 2005, Ap.J., 634, 161
Kauffmann, G., et al., 2003, MNRAS, 341.,33
Kewley, L.J., et al., 2001, ApJ., 556, 121.
Kewley, L.J., et al., 2006, MNRAS, 372, 961
Kraemer, S.B. et al., 2004, ApJ 607, 794
Netzer, H., et al., 2006, A&A, 453,525
Panessa, F., et al., 2006, A&A, 455,173
Ptak, A., et al., 2006, Ap.J., 637, 147